



上海交通大学

SHANGHAI JIAO TONG UNIVERSITY

The 11th International Conference of ICE Reliability Technology

Coupled tribology and vibration characteristics of reciprocating friction pairs of diesel engines



Yi Cui, Shuo Liu, Chuanbin Zhang

Feb. 19, 2023

Content

01

Introduction

02

Numerical model

03

Results & analysis

04

Conclusions



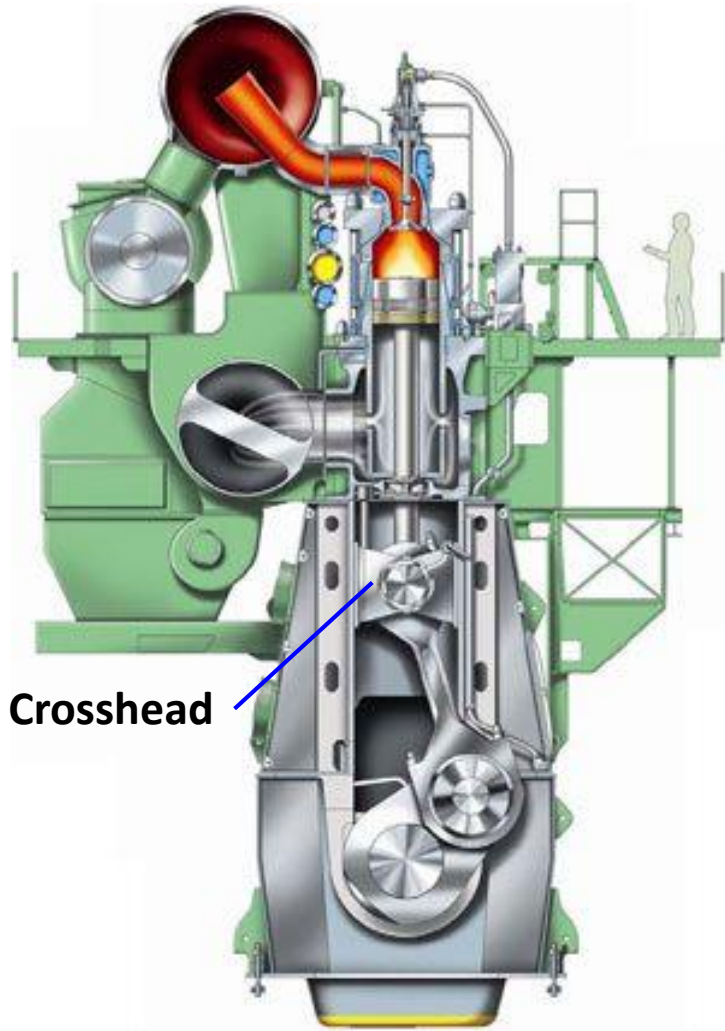
PART 01

Introduction





Introduction



Background

- **Low-speed two-stroke marine diesel engines** are widely used as propulsion power in large ships, with the advantages in:
 - High thermal efficiency; power; and reliability.

Crosshead-guides reciprocating friction pairs

- Side force mainly comes from crosshead.
- Crosshead-guides pair would cause **great friction loss** of engines.
- The impact of crosshead contributes most of the **vibration and noise** in some engines.



Introduction

Background

- Modern **internal combustion engines** are developing in the direction of high efficiency and reliability.

Piston-liner reciprocating friction pairs

- Side force mainly comes from piston.
- Piston-liner pairs bring about nearly **50% of all the frictional loss** in an ICE.
- The piston slap accounts for **about 9% of the total vibration energy**, and about **12% of the total noise**.

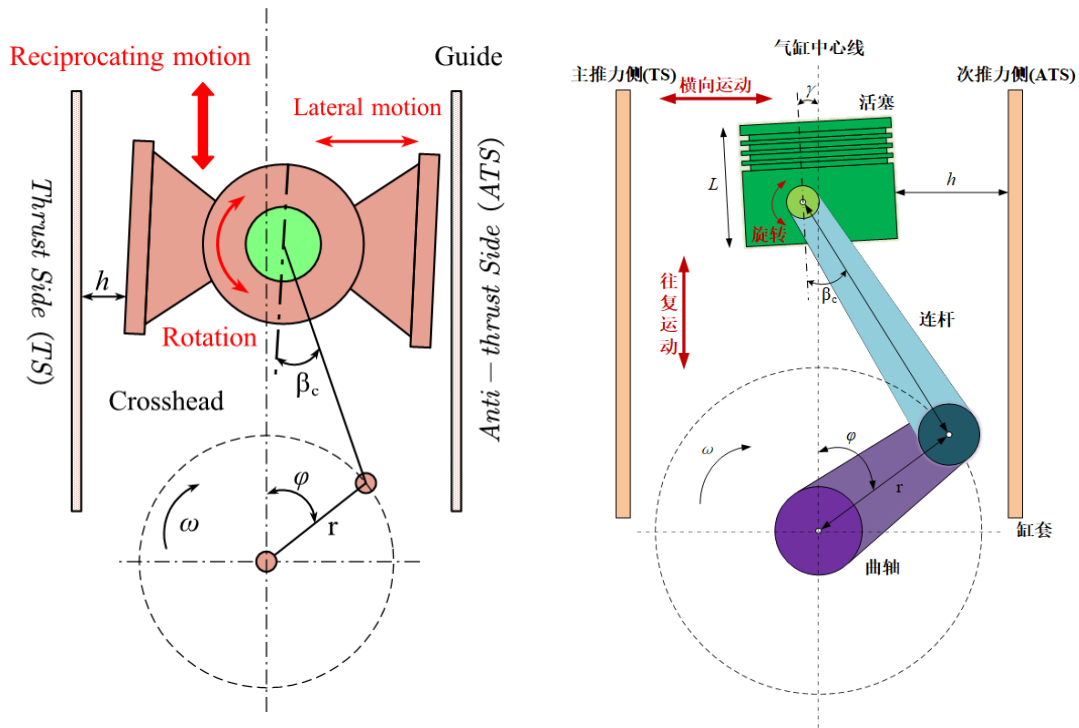




Introduction

Due to the clearance, **reciprocating motion** often accompanied by **secondary motions**:

Lateral motion, and rotational motion.



Oil film thickness

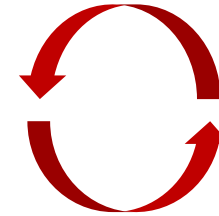
Dynamic responses

Determined by:

1. Secondary motion
2. Surface vibration
3. Elastic deformation
4. Temperature

Driven by:

1. Normal oil film forces
2. Tangential shear forces



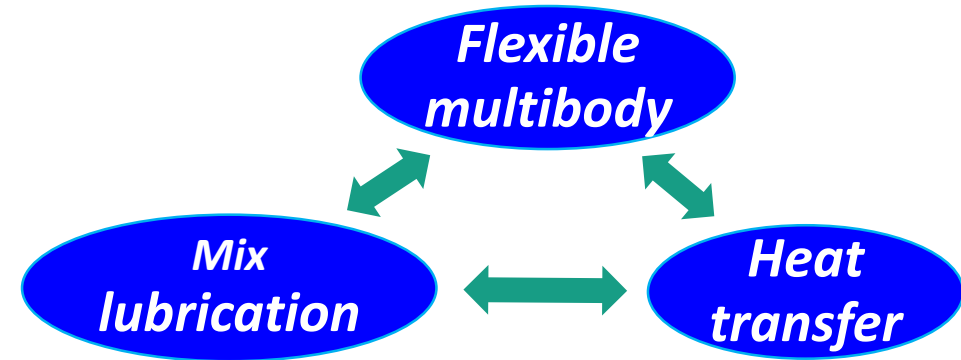


Introduction

Current studies

- The lubrication calculation is based on the finite difference method, which is **difficult to deal with complex lubrication boundaries** such as the piston skirt.
- In the coupled multiphysics calculation including temperature, lubrication, dynamics, etc., **each physics is solved separately**. Computational efficiency and convergence performance are low.
- The multi-flexible body systems are simplified with the condensation of degrees of freedom, which is **hard to deal with high-frequency vibrations**.

New tribo-dynamic model



Mixed lubrication

Average Reynolds Equation + G-T asperity contact theory.

Spatial rigid-flexible multibody system

Pairs related to reciprocating friction pairs are treated as **flexible bodies**.



PART 02

Numerical model





Numerical model

Tribo-dynamic coupling model

1. Mixed lubrication
of reciprocating friction
pairs

2. Rigid-flexible
multibody system-
ANCF method

3. Computational
algorithm

Spatial discretization by
FEM;
Time discretization by
Generalized α .



Numerical model

Mixed lubrication of reciprocating friction pairs

- **Governing equation**

$$\nabla_t \cdot (\rho h_p \bar{\mathbf{v}}_{av}) + \phi_c \frac{\partial(\rho h_p)}{\partial t} = 0 \quad \rho c_p \frac{\partial T}{\partial t} + \rho c_p \mathbf{u} \cdot \nabla T + \nabla \cdot (-\lambda \nabla T) = Q_{vd}$$

- **Boundary condition**

$$p(x, y) = 0, (x, y) \in \Gamma$$

$$T|_{L=0} = T_p, T|_{L=h} = T$$

- **Oil film thickness**

$$h_p = c + h_{prof} + h_s + d_p + d_l + d_{pre}$$

Secondary motion

Deformation

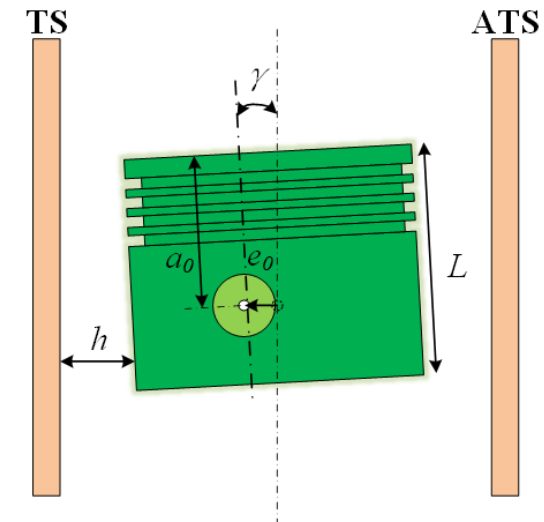
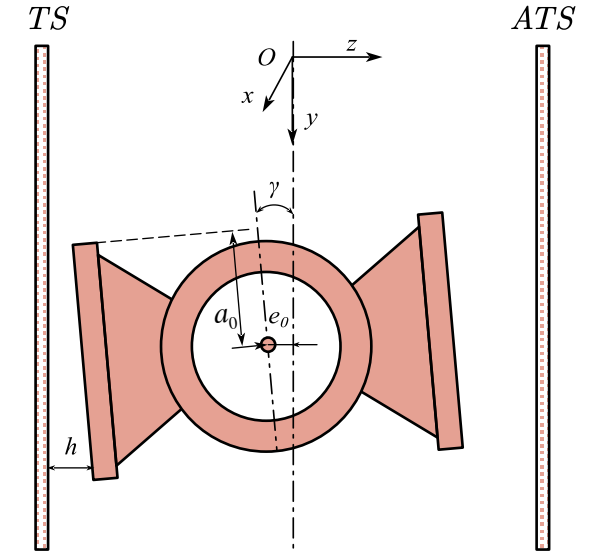
(contact, vibration)

Deformation

(thermal, preload)

- **Asperity contact**

$$p_c(h) = KE' F_{5/2}(H_\sigma)$$





Numerical model

Finite element solution

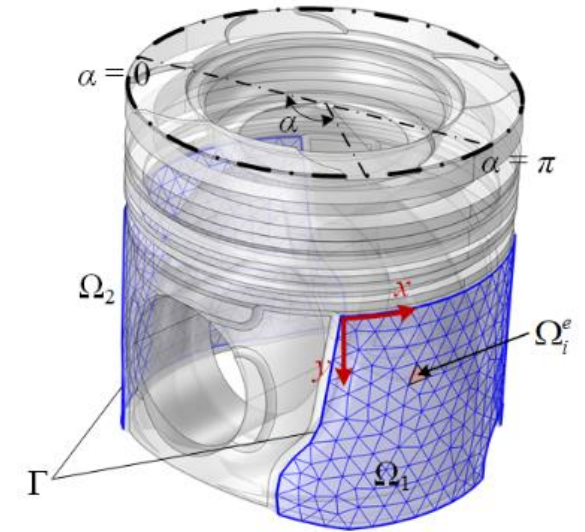
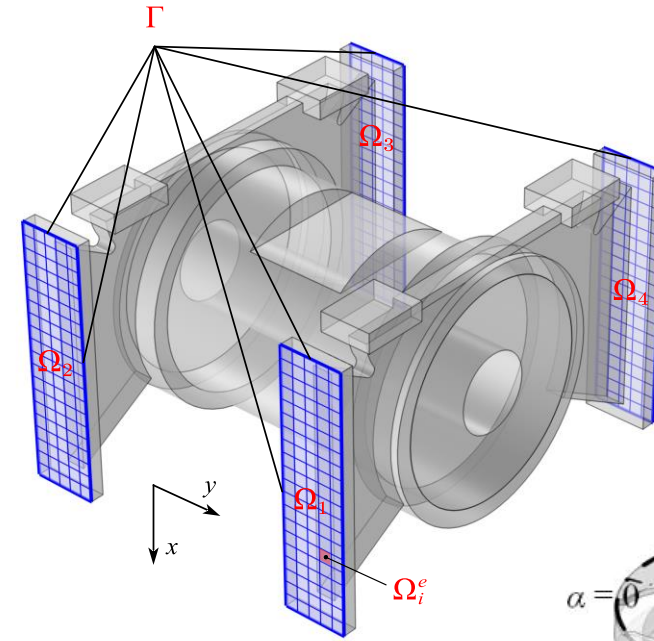
- Weak form of equivalent integral

$$\int_{\Omega} [(\rho h \bar{\mathbf{v}}_{av}) \cdot \nabla_t \delta p] d\Omega - \int_{\Omega} \left[\phi_c \frac{\partial(\rho h)}{\partial t} \delta p \right] d\Omega = 0$$

- Algebraic equations of FEM

$$\sum_e \mathbf{K}^e \mathbf{P} = \sum_e \mathbf{F}^e$$

$$\left\{ \begin{array}{l} \mathbf{K}^e = - \int_{\Omega^e} \phi_i \frac{\rho h^3}{12\mu} [(\nabla_t \mathbf{N}^T)^T \nabla_t \mathbf{N}^T] d\Omega \\ \mathbf{F}^e = \int_{\Omega^e} \left\{ \rho h (\nabla_t \mathbf{N}^T)^T \left[\frac{1}{2} \phi_c (\mathbf{I} - \mathbf{n}_r \mathbf{n}_r^T) (\mathbf{v}_w + \mathbf{v}_b) \right. \right. \\ \left. \left. + \frac{1}{2} \phi_s \frac{\sigma}{h} (\mathbf{I} - \mathbf{n}_r \mathbf{n}_r^T) (\mathbf{v}_w - \mathbf{v}_b) \right] - \phi_c \frac{\partial(\rho h)}{\partial t} \mathbf{N} \right\} d\Omega \end{array} \right.$$

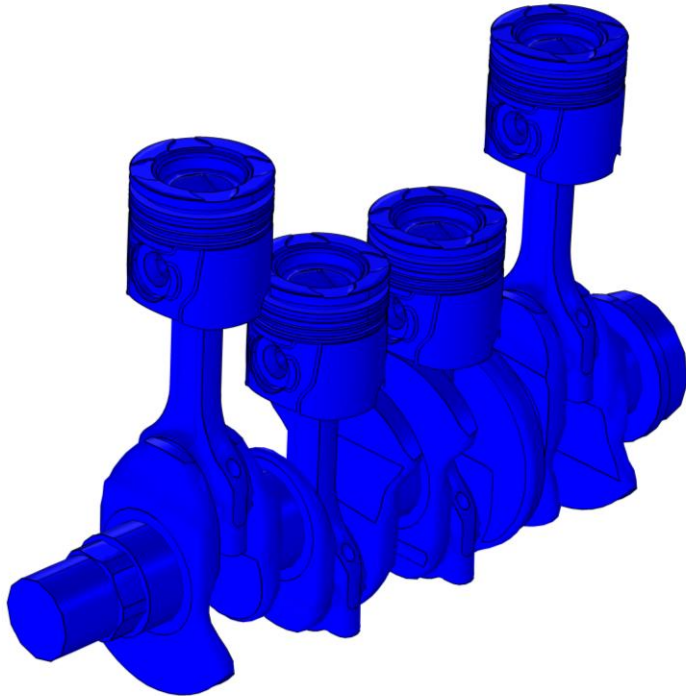




Numerical model

Rigid-flexible multibody system

- Pairs related to reciprocating friction pairs are treated as **flexible bodies**.
- Other parts are treated as **rigid bodies**.



Governing equations of motion

$$\begin{cases} \mathbf{M}\ddot{\mathbf{q}} + \mathbf{C}\dot{\mathbf{q}} + \mathbf{K}\mathbf{q} + \Phi_{\mathbf{q}}^T(\mathbf{q})\boldsymbol{\lambda} = \mathbf{Q} \\ \Phi(\mathbf{q}, t) = 0 \end{cases}$$

Nonlinear algebraic equations by generalized- α .

$$\mathbf{M}\ddot{\mathbf{q}}_{n+1-\alpha_m} + \mathbf{C}\dot{\mathbf{q}}_{i+1-\alpha_f} + \mathbf{K}\mathbf{q}_{i+1-\alpha_f} + \Phi_{\mathbf{q}}^T(\mathbf{q}_{i+1-\alpha_f})\boldsymbol{\lambda}_{n+1} = \mathbf{Q}(t_{i+1-\alpha_f})$$

$$\ddot{\mathbf{q}}_{n+1-\alpha_m} = (1-\alpha_m)\ddot{\mathbf{q}}_{n+1} + \alpha_m\ddot{\mathbf{q}}_n$$

$$\dot{\mathbf{q}}_{n+1-\alpha_f} = (1-\alpha_f)\dot{\mathbf{q}}_{n+1} + \alpha_f\dot{\mathbf{q}}_n$$

$$\mathbf{q}_{n+1-\alpha_f} = (1-\alpha_f)\mathbf{q}_{n+1} + \alpha_f\mathbf{q}_n$$

$$t_{n+1-\alpha_f} = (1-\alpha_f)t_{n+1} + \alpha_ft_n$$

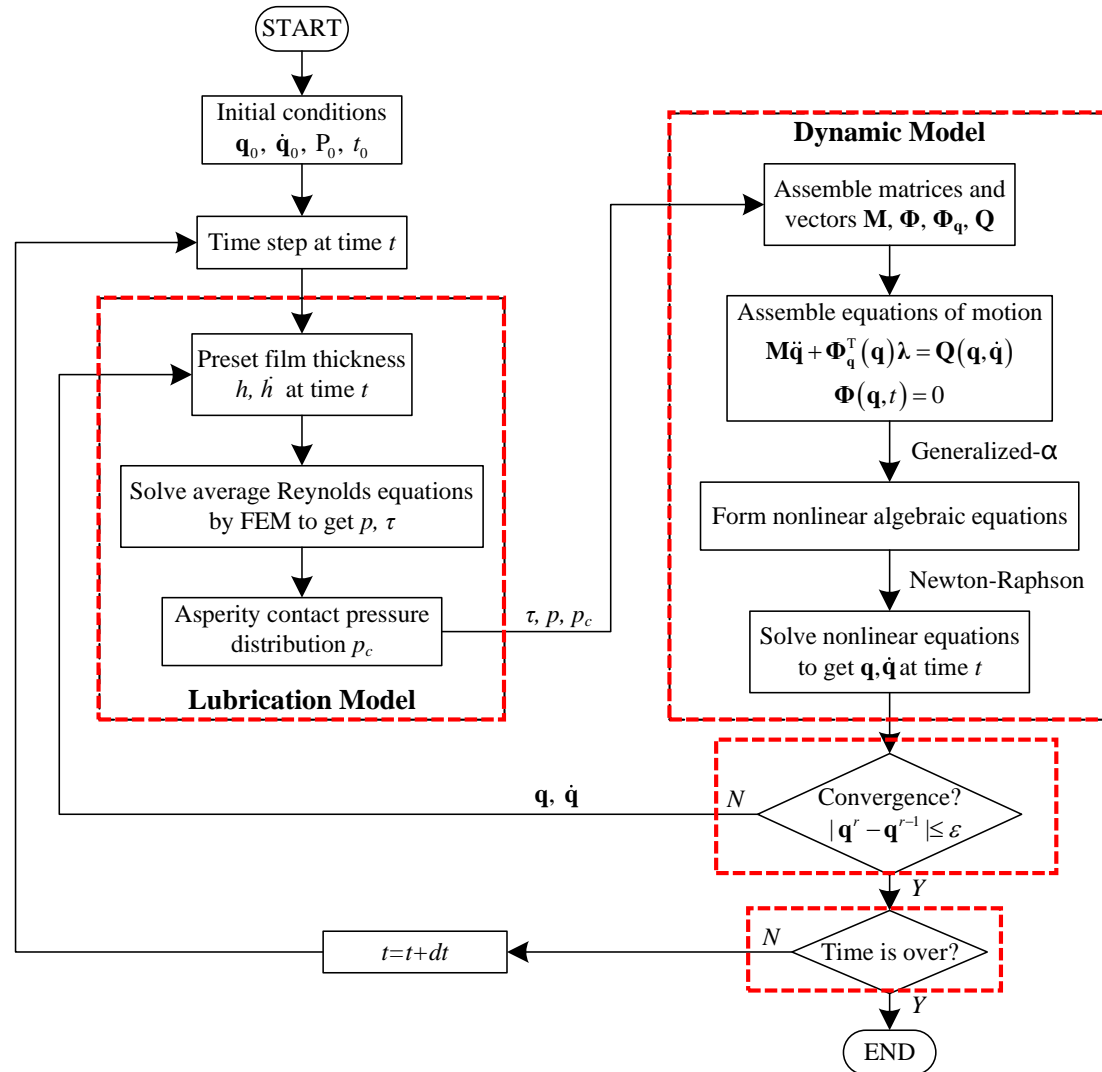
$$\ddot{\mathbf{q}}_{n+1} = \frac{1}{\beta\Delta t^2}(\mathbf{q}_{n+1} - \mathbf{q}_n) - \frac{1}{\beta\Delta t}\dot{\mathbf{q}}_n - \left(\frac{1}{2\beta} - 1\right)\ddot{\mathbf{q}}_n$$

$$\dot{\mathbf{q}}_{n+1} = \frac{\gamma}{\beta\Delta t}(\mathbf{q}_{n+1} - \mathbf{q}_n) - \left(\frac{\gamma}{\beta} - 1\right)\dot{\mathbf{q}}_n - \Delta t\left(\frac{\gamma}{2\beta} - 1\right)\ddot{\mathbf{q}}_n$$



Numerical model

Computational algorithm



- **Lubrication model**

- Oil film thickness is calculated by dynamic responses.
- Oil film forces would be embedded into spatial rigid-flexible multibody system.

- **Dynamic model**

- The motion, deformation, and vibration are solved by the generalized- α method.
- Dynamic responses would return to correct the oil film thickness.
- In one time step, the tribo-dynamic coupling model is solved iteratively.
- By time stepping, coupling model can be solved.



PART 03

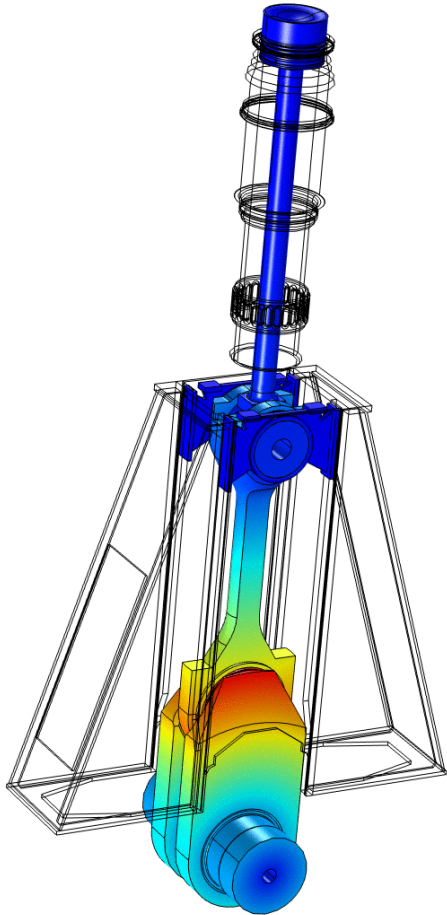
Results & analysis



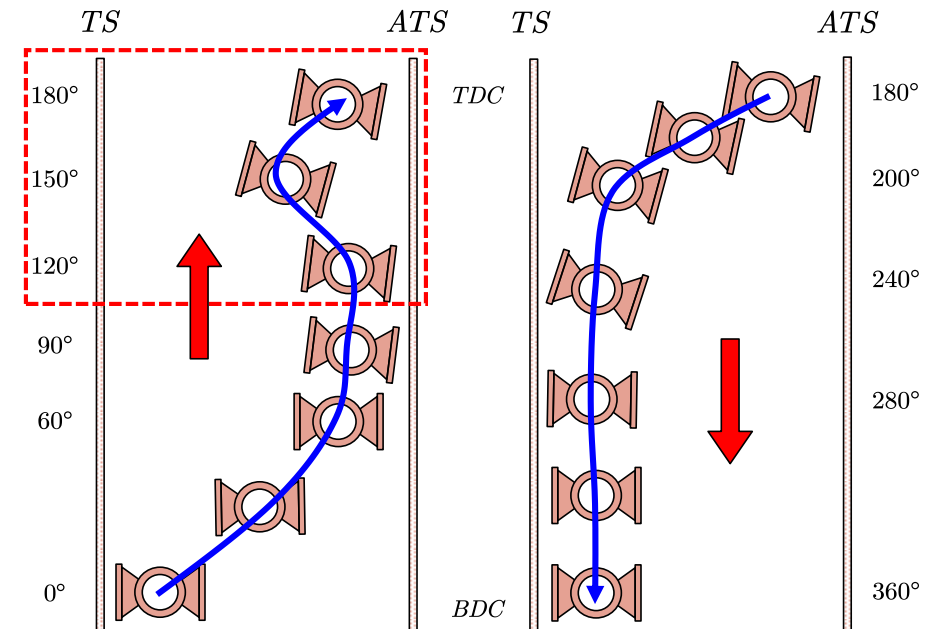
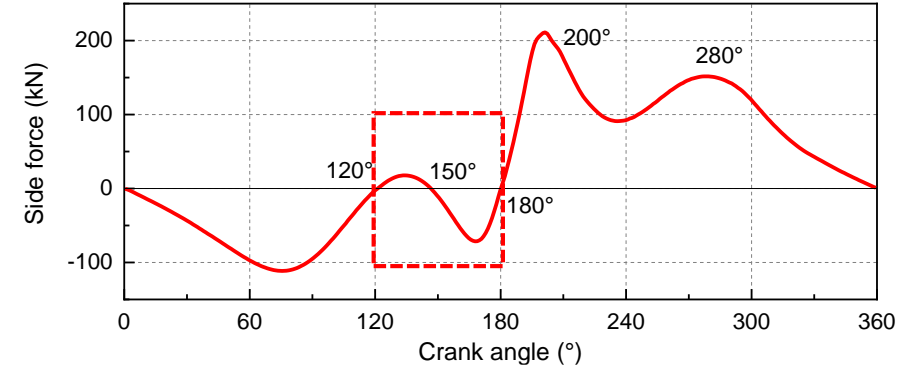


Results & analysis --- Crosshead/Guides pairs

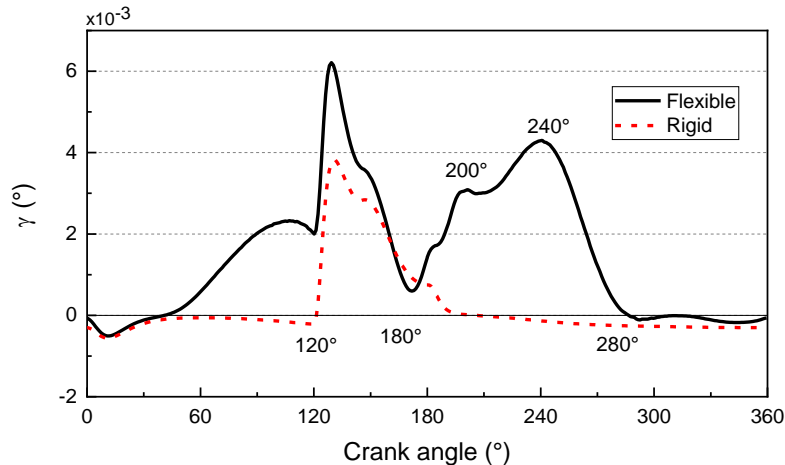
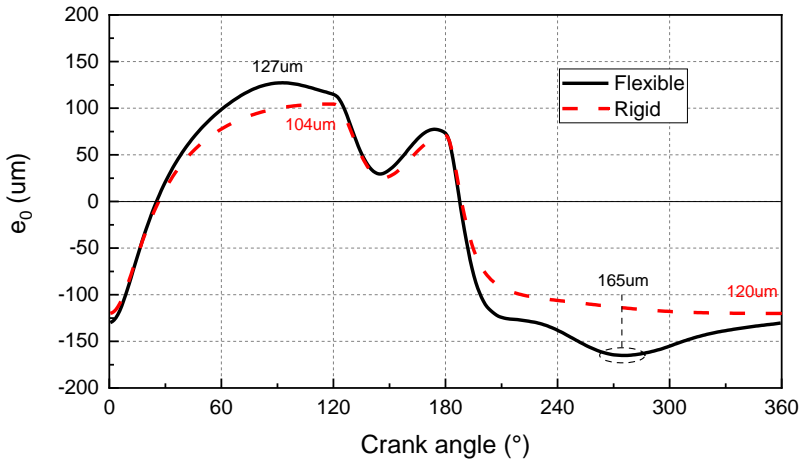
Analysis and comparison of dynamic results



- **Side force**
 - obtained by integrating the oil film pressure and asperity contact pressure.
- **Motion posture**
 - obtained by combining reciprocating motion and secondary motion together.
 - crosshead swings left and right between the TS and ATS during $120^\circ \sim 180^\circ$ CA, due to reciprocating inertial forces.

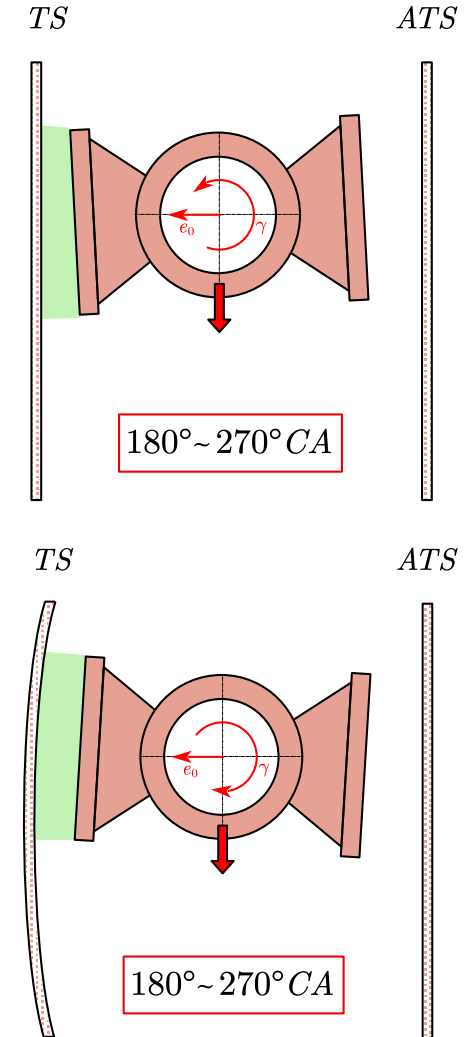


Analysis and comparison of dynamic results

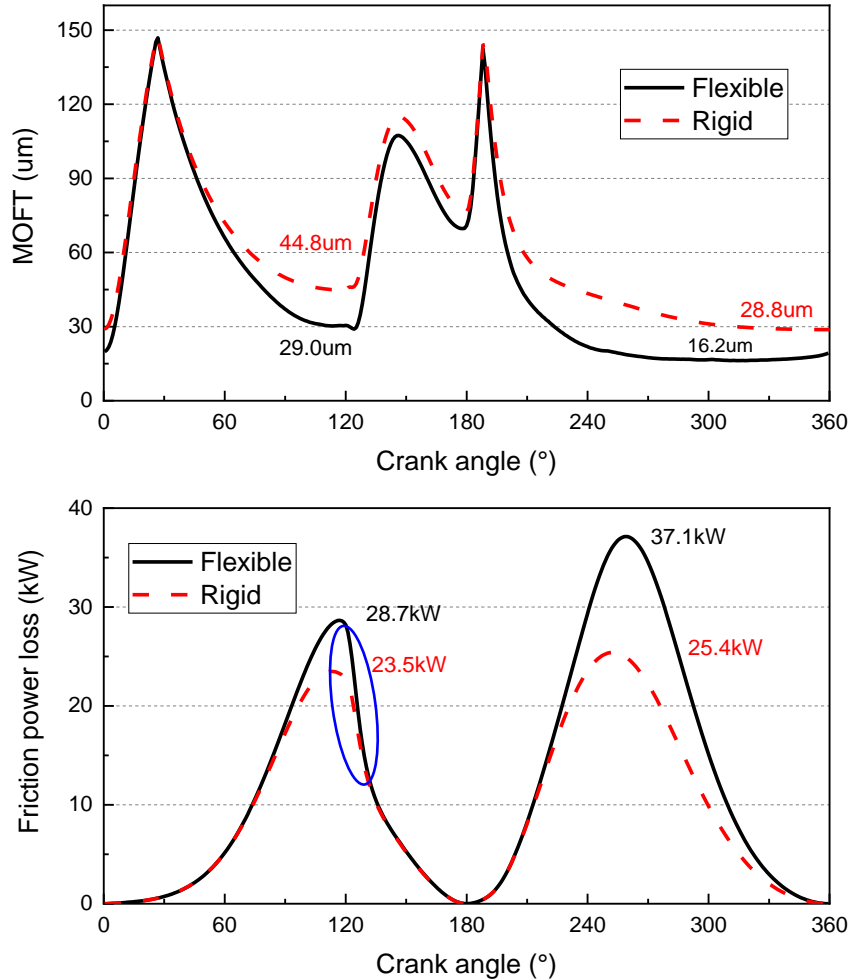


More intense secondary motion

- **Lateral displacement** of crosshead is much larger, with the difference up to 37%.
- Crosshead **rotates clockwise** with a large angle during the period of $180^\circ \sim 270^\circ CA$.
- Main reason for the clockwise is due to the deformation of guides.
- flexible body modeling describes the secondary motion of crosshead better.
- And provides **more accurate boundary conditions** for tribological calculations.

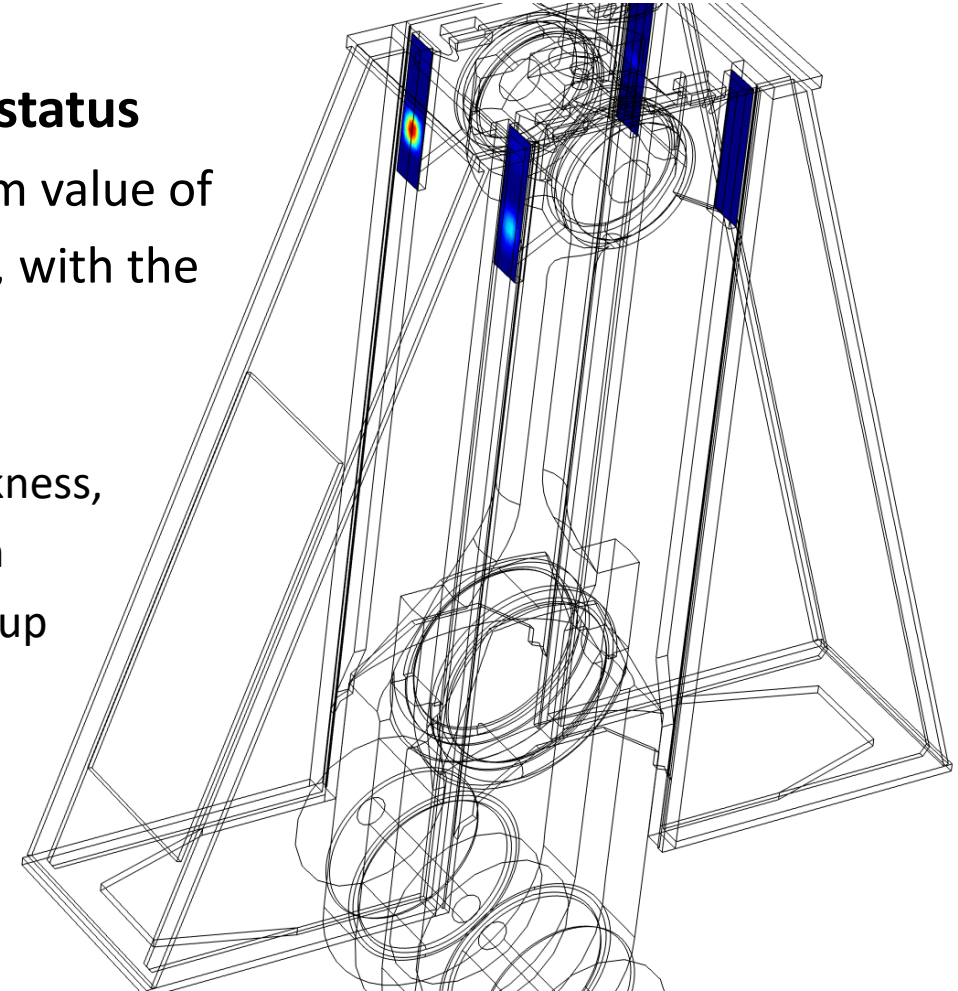


Analysis and comparison of lubrication results

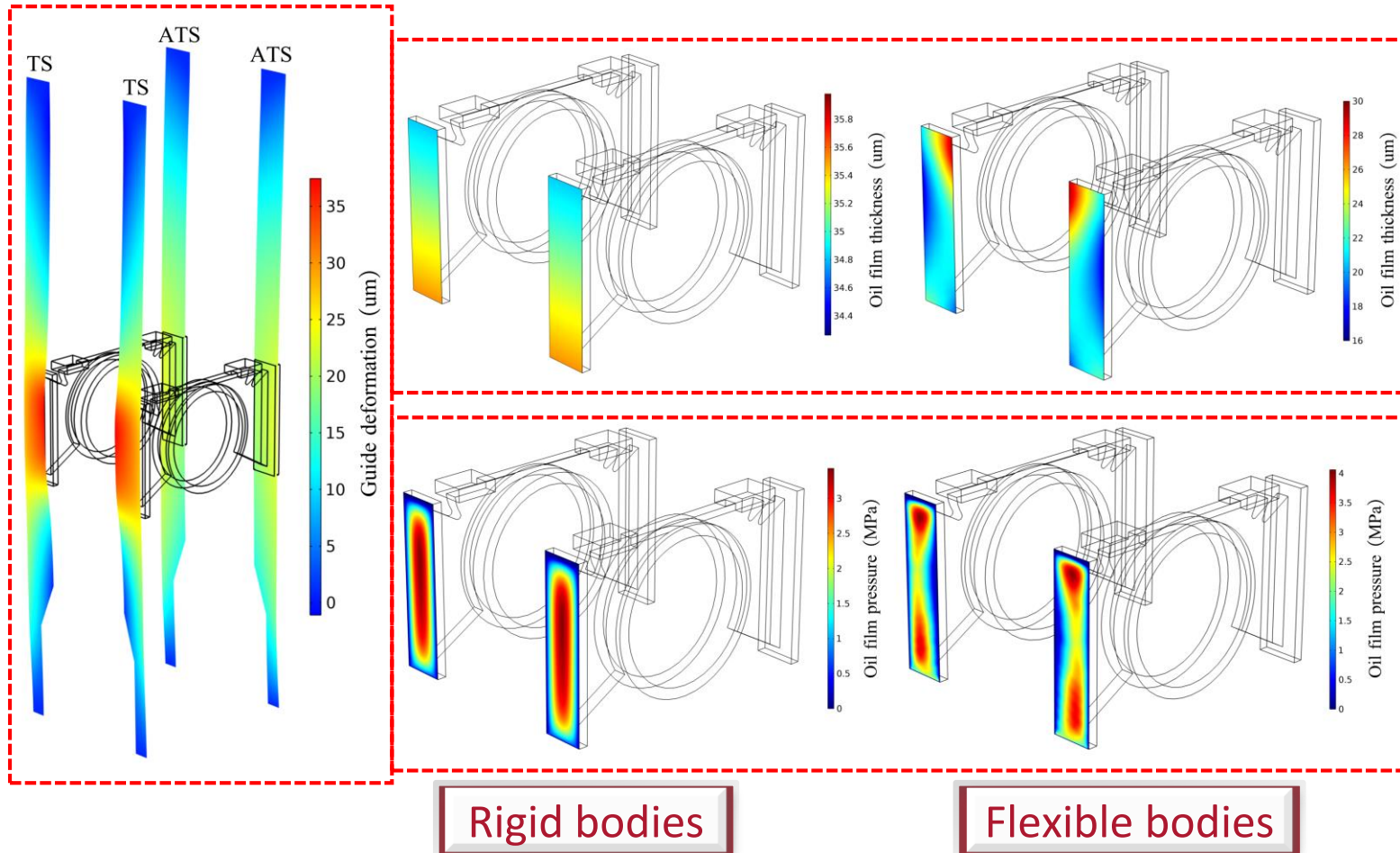


More worse lubrication status

- **MOFT** with the minimum value of 16.2μm is much smaller, with the difference up to 44%.
- Owing to smaller film thickness, **friction power loss** is much larger, with the difference up to 34%.
- During 120°~135°CA, friction power loss reduce sharply due to increased oil film thickness.



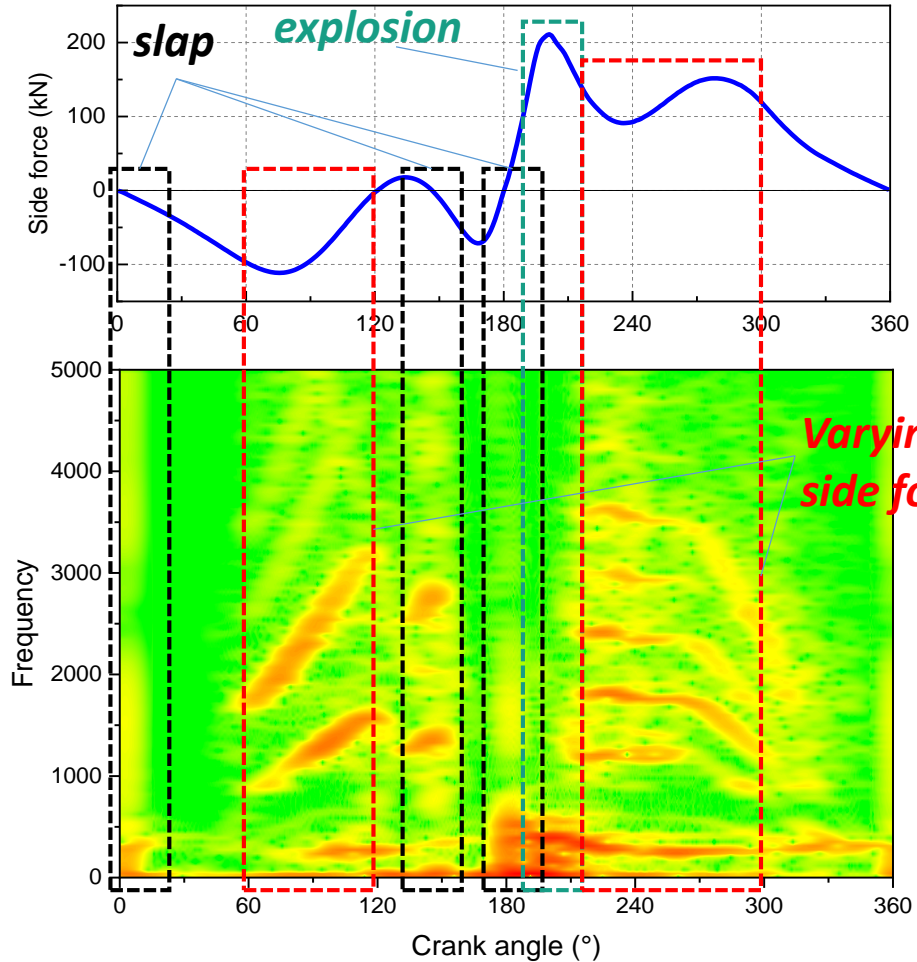
Fields comparison at the moment of maximum side force



Fields comparison at 280°CA

- The maximum **deformation of guides is near 40um**, which is in the same order of film thickness.
- Considering the deformation, local clearance and film thickness is smaller.
- New phenomenon occurs that **two pressure peaks** situated in the upper half and the lower half of lubrication domain.

Transmission characteristics of vibration signals



- **Slap vibrations**

Wide vibration frequency bands are excited within narrow CA ranges.

- 0 °CA, BDC;
- 150 °CA, before TDC;
- 180 °CA, TDC.

- **Vibration by explosion pressure**

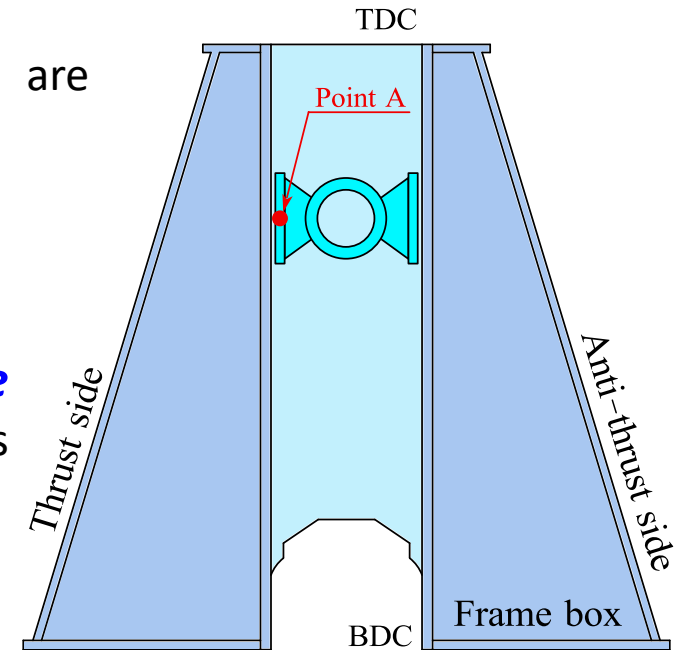
Side force of crosshead increases rapidly and reaches the maximum.

- 200 °CA, after TDC.

- **Vibration by lateral forces**

No reversing behavior of crosshead, and slap energy is as low as zero. Periodical side force excites the vibration.

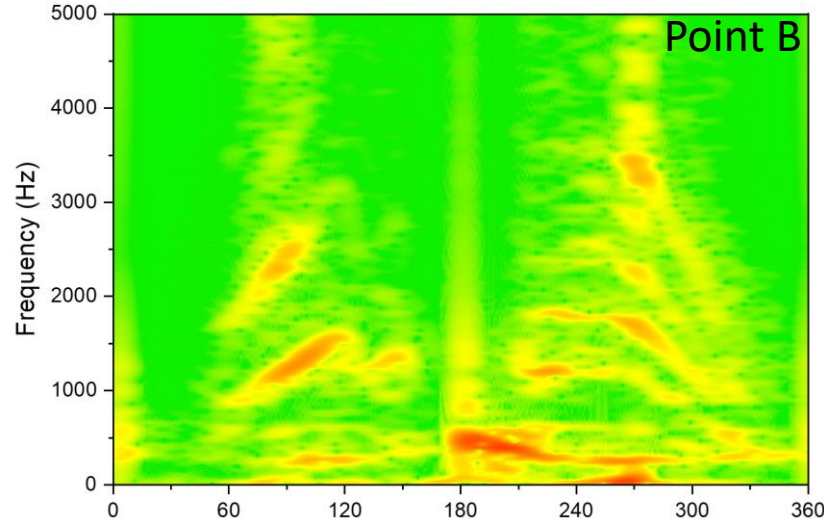
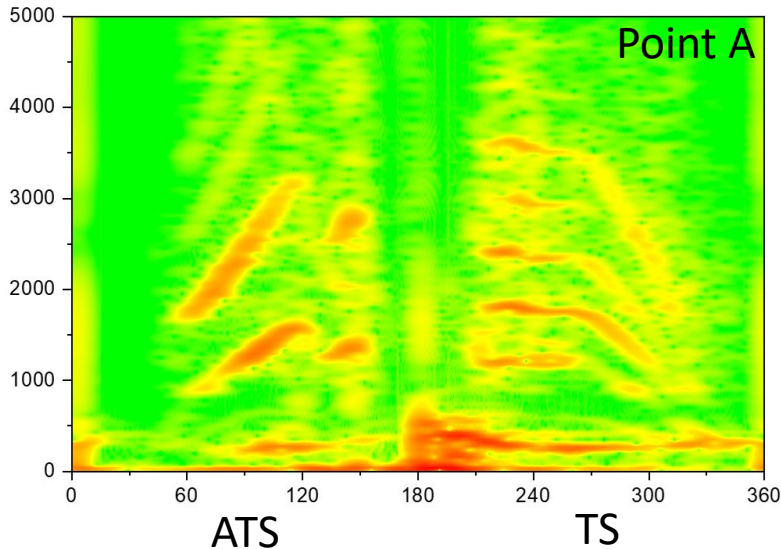
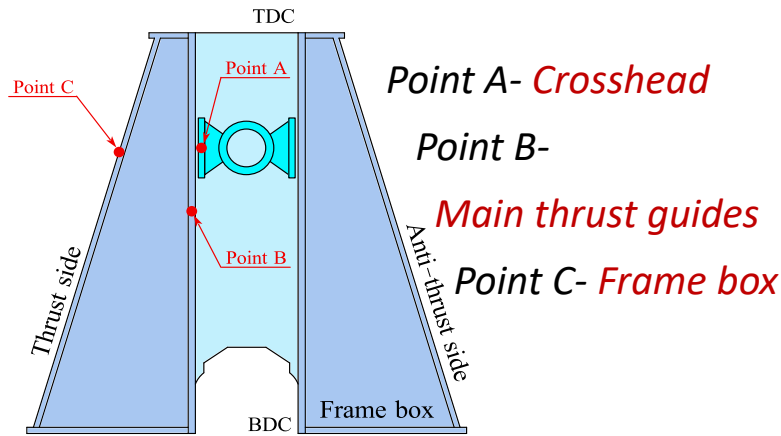
- 60 °~120°CA;
- 200 °~300°CA.





Results & analysis --- Crosshead/Guides pairs

Transmission characteristics of vibration signals

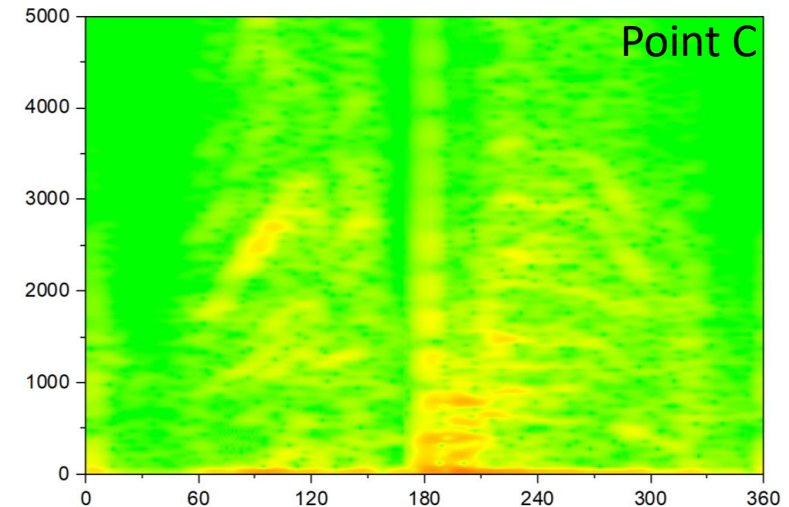


Vibration transmitted to guides

- Vibrations have been attenuated to a certain extent due to oil film.
- When crosshead is pressed to ATS, vibrations received by main thrust guides are greatly attenuated.
- At 280°C, peak side force leads to a strong guides vibration.

Vibration transmitted to Surface

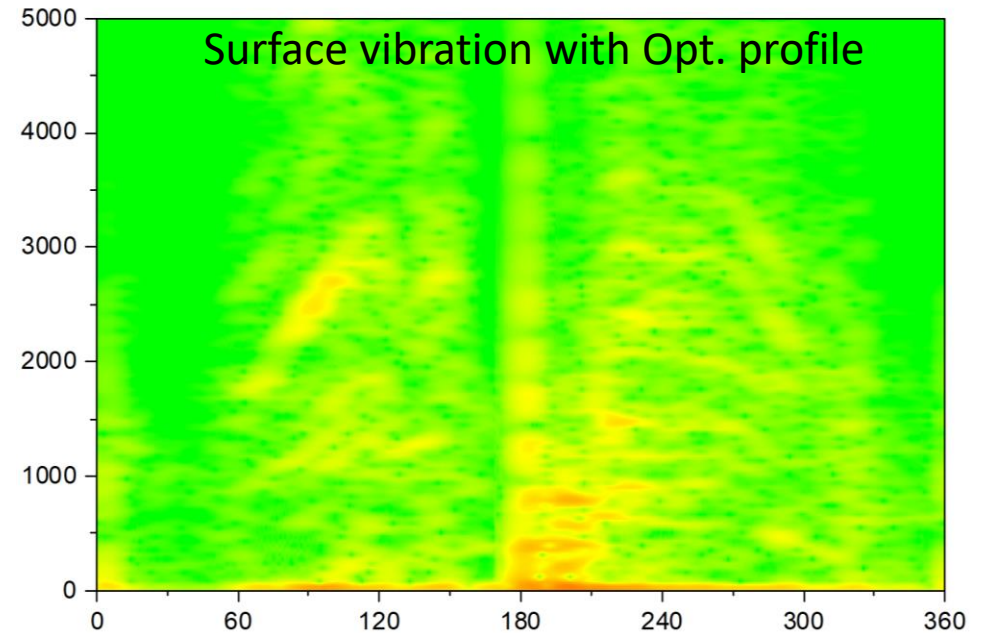
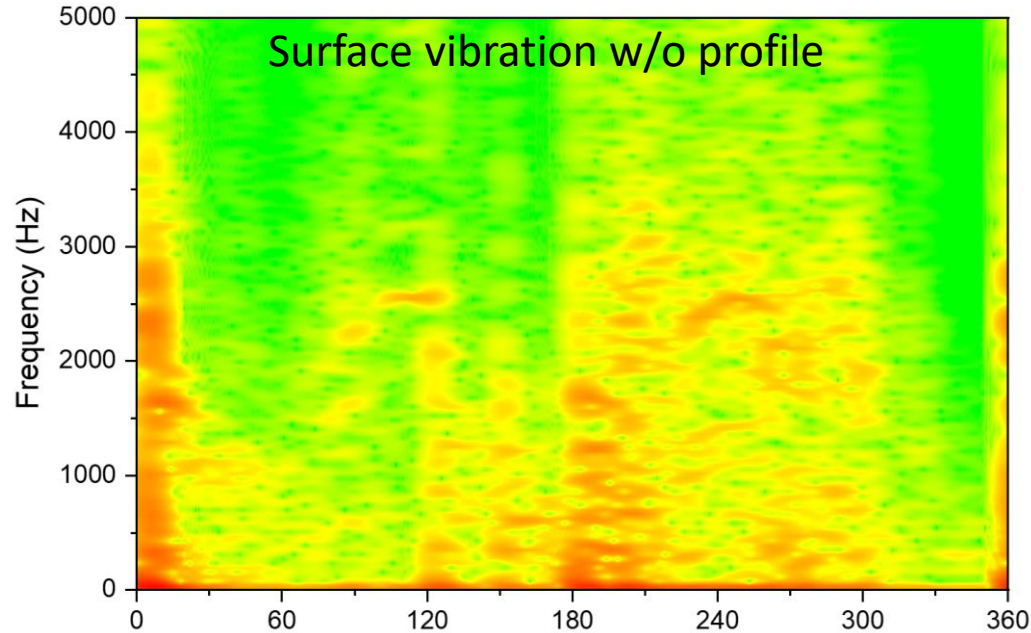
- Vibrations are further attenuated due to the internal damping and fixed boundary of frame box.
- Vibration mainly caused by slapping at the TDC and the gas explosion pressure.





Results & analysis --- Crosshead/Guides pairs

Transmission characteristics of vibration signals



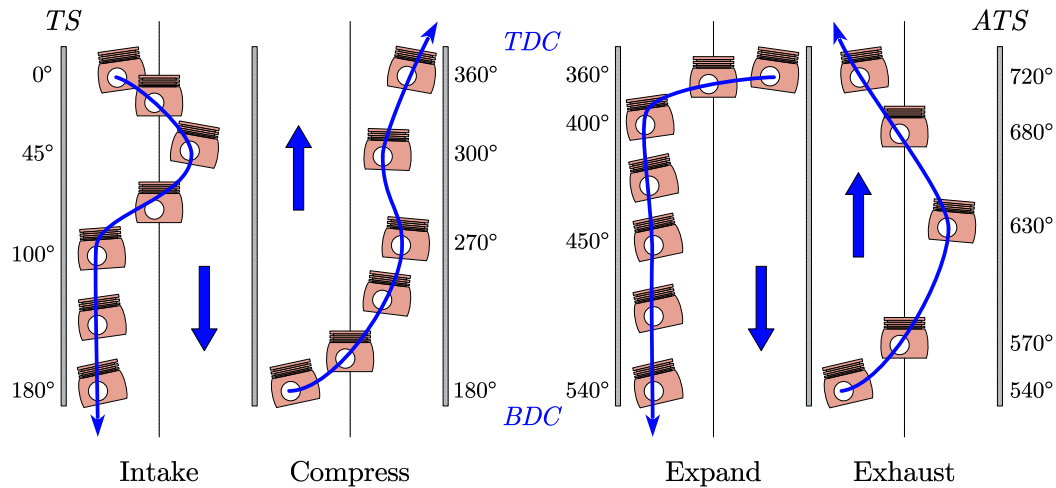
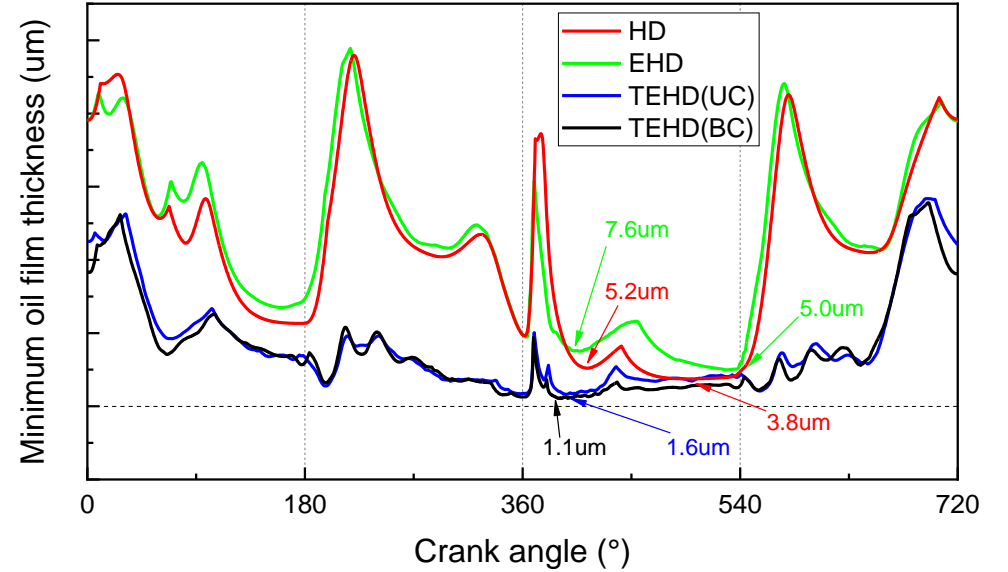
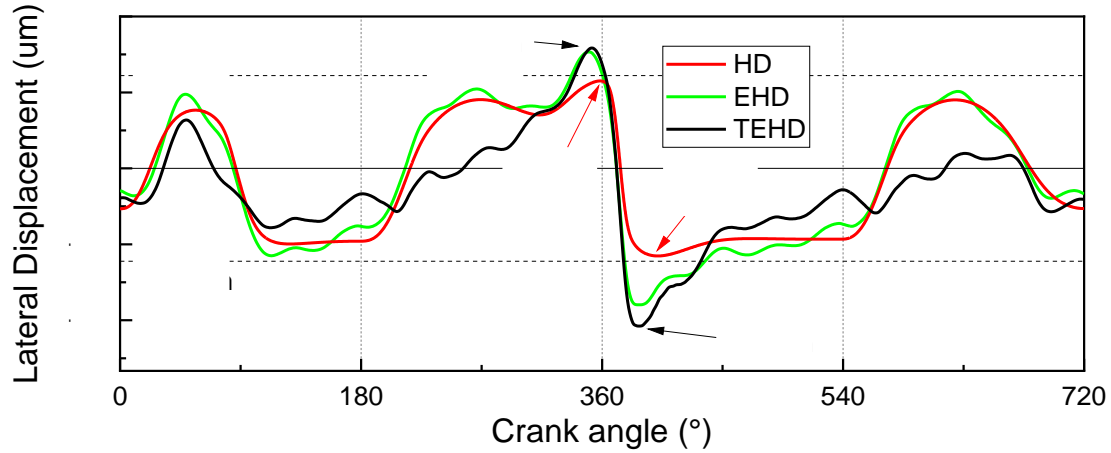
Conclusions

- Specific profile of crosshead can greatly reduce the vibration energy of each frequency band caused by the **crosshead slapping**, and reduce the frame box **vibration excited by the lateral forces** as well.
- Further study about vibration reduction, the strategy would focus on reducing the low-frequency vibration energy near the TDC.



Results & analysis --- Piston/Liner pairs

Analysis and comparison of dynamic results

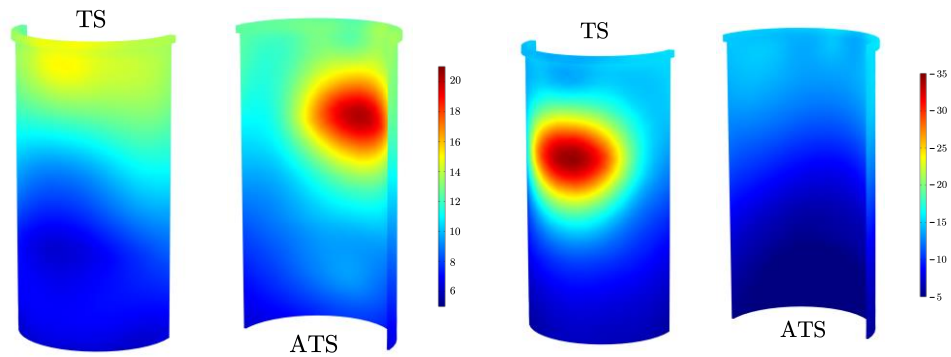
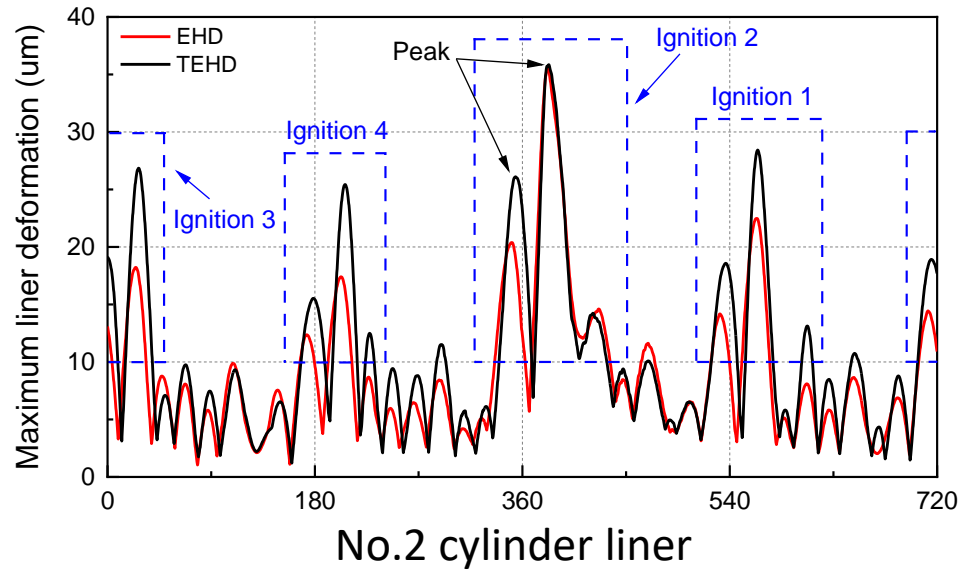


- Around 360°CA, the lateral displacement of piston reaches the maximum value on the ATS and TS sides respectively.
- Compared with rigid body, better lubrication status for flexible body.
- Considering the vibration, heat transfer and deformation in TEHD model, there exists 80.2% difference of the maximum values of lateral displacement with rigid model.



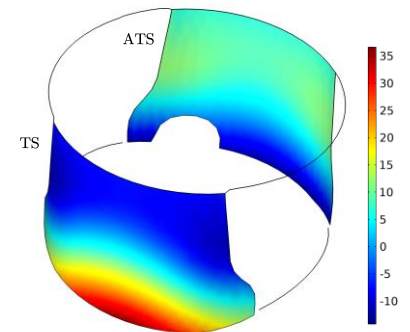
Results & analysis --- Piston/Liner pairs

Analysis and comparison of dynamic results

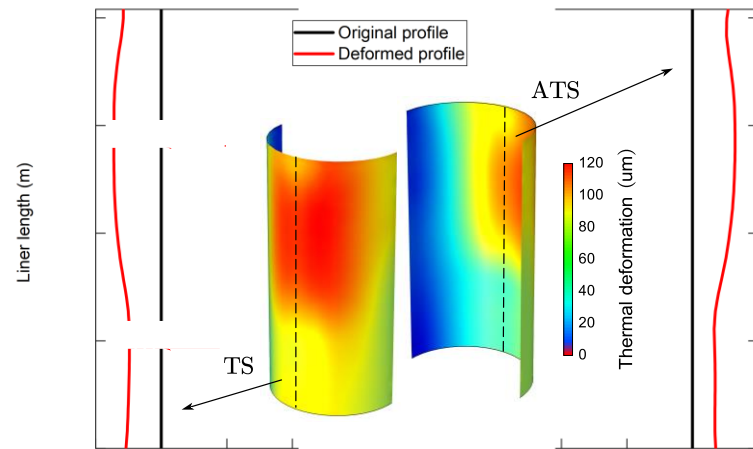
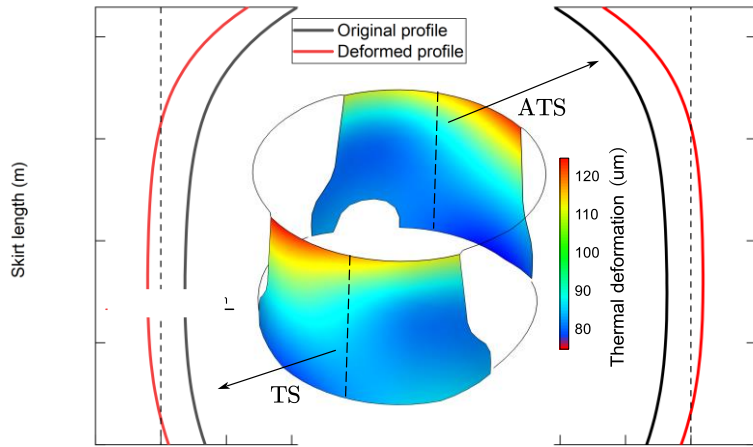


Maximum deformation of liners

- Corresponding to the firing order of 1-3-4-2, there would exist **four peaks** of maximum liner deformation in one cycle.
- Affected by the vibration of engine, the maximum liner deformation **fluctuates** in one cycle.
- During 350-380°C_A, the position of maximum deformation is changed **from ATS side to TS side**.
- The maximum elastic deformation of piston and liner is **45.8um** and **36.9um**, respectively.



Analysis and comparison of lubrication results



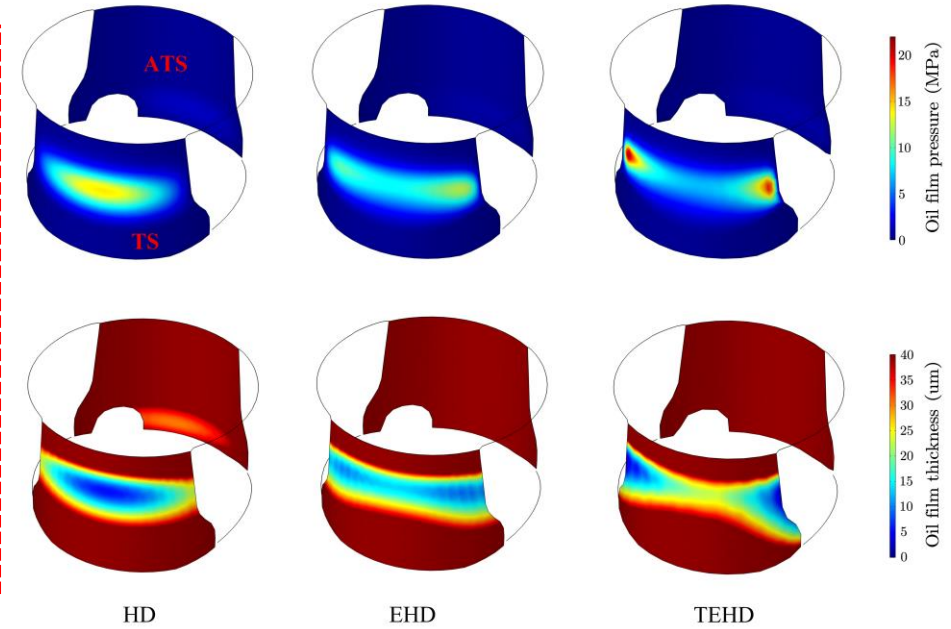
Thermal deformation of cylinder liners at TS and ATS (um)

- Influence of heat**

- Thermal deformation of piston skirt is 74.4-123.0um.
- Thermal deformation of liner in ATS side is 72.8-108.6um.

Liner length (m)

Skirt length (m)

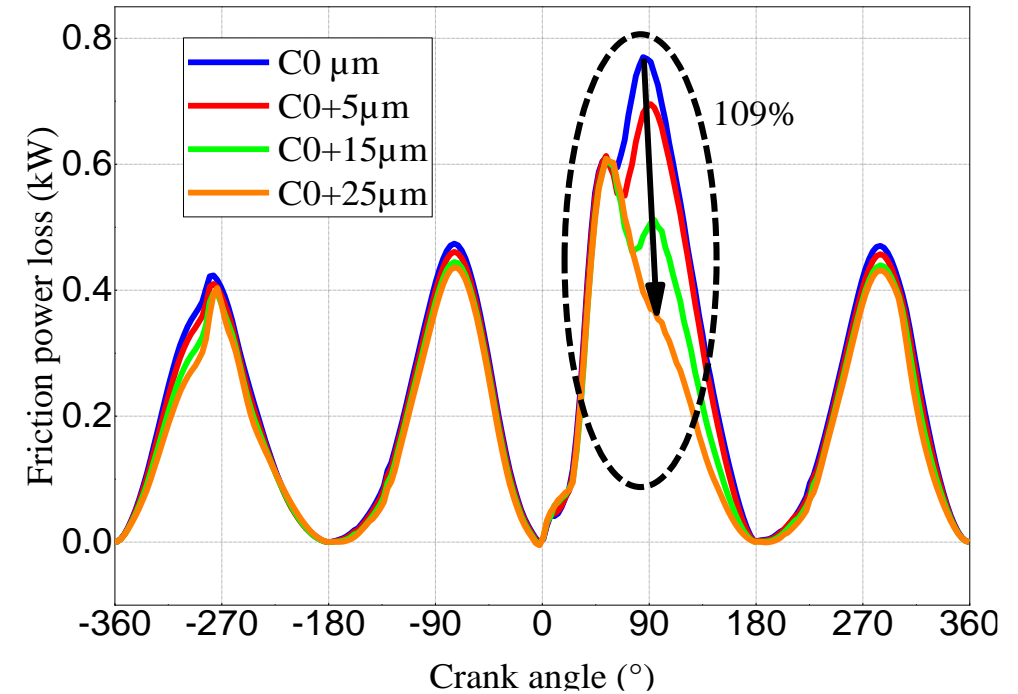
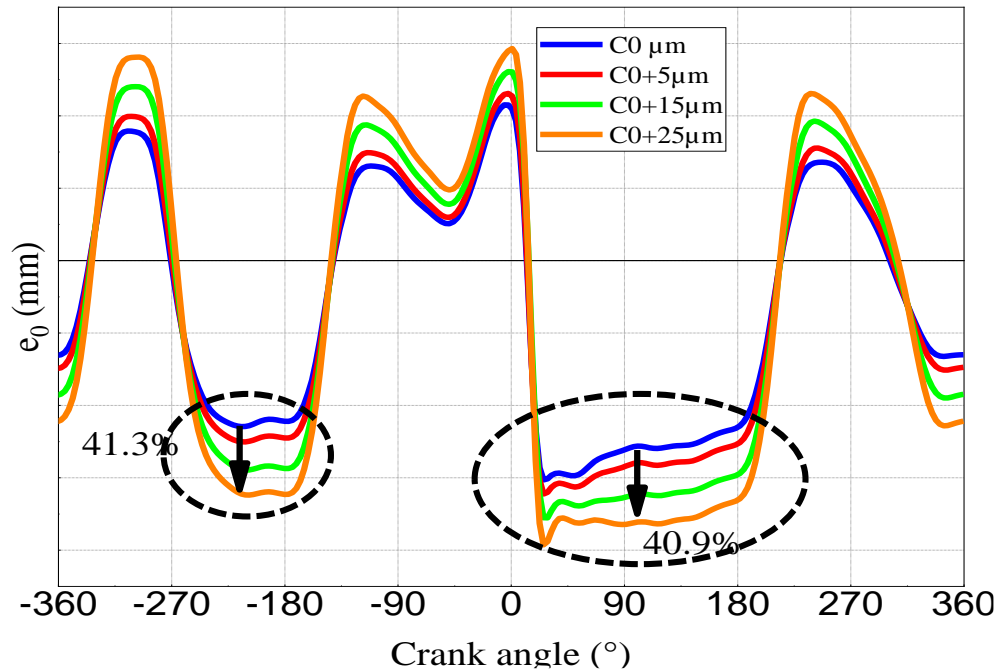


- At the moment of largest lateral force (380°CA), the MOFT of TEHD model is **1.1um**, which is **88% lower** than that of EHD model; the peak pressure is **21.9MPa**, which is **78% higher** than that of EHD model.



Results & analysis --- Piston/Liner pairs

Influences of fit clearance



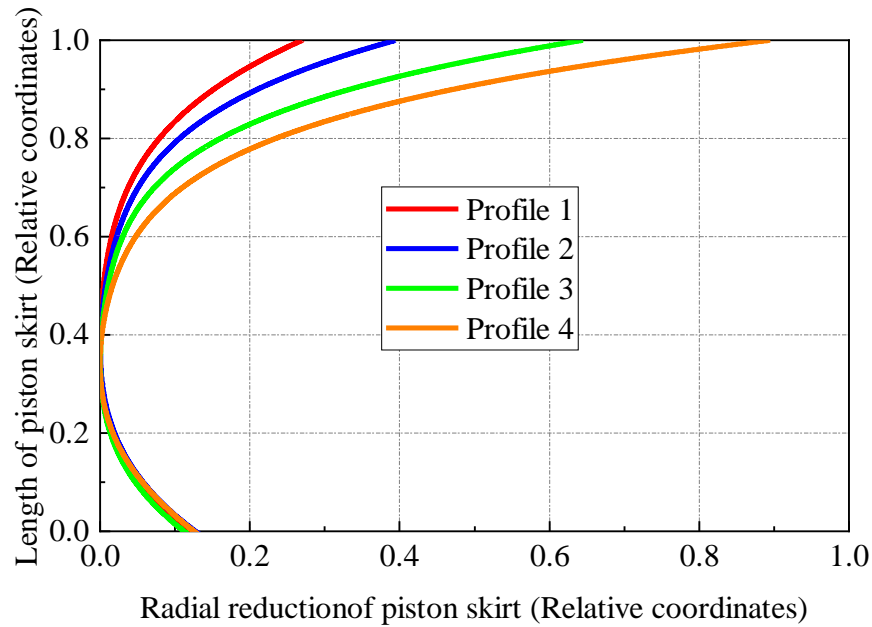
Increase the clearance

- Lateral displacement and rotation angle are **more intense**.
- MOFT increases and **friction power loss decreases** obviously.

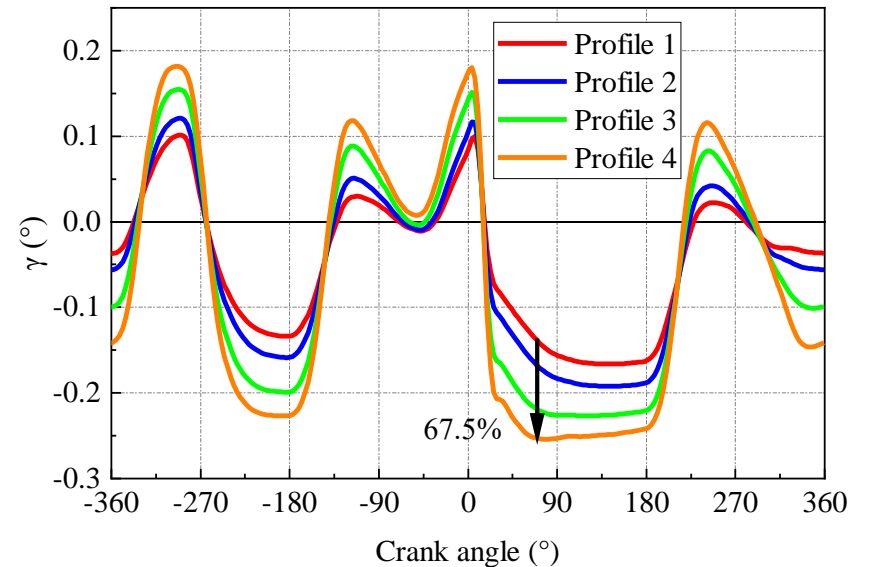
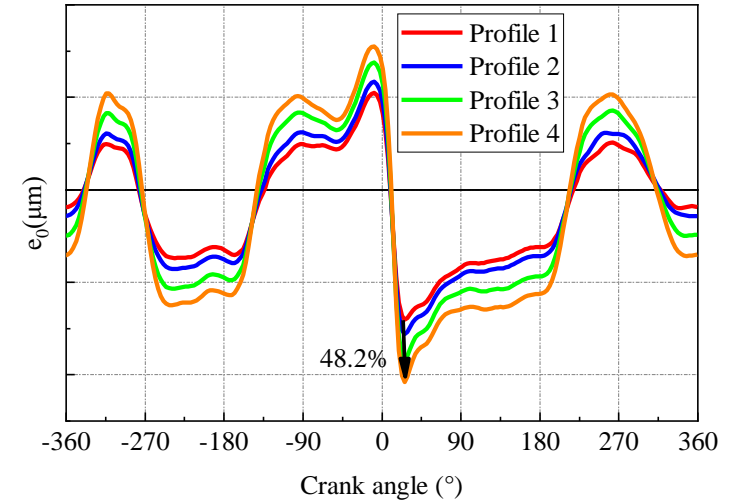


Results & analysis --- Piston/Liner pairs

Influences of radial reductions on the upper skirt



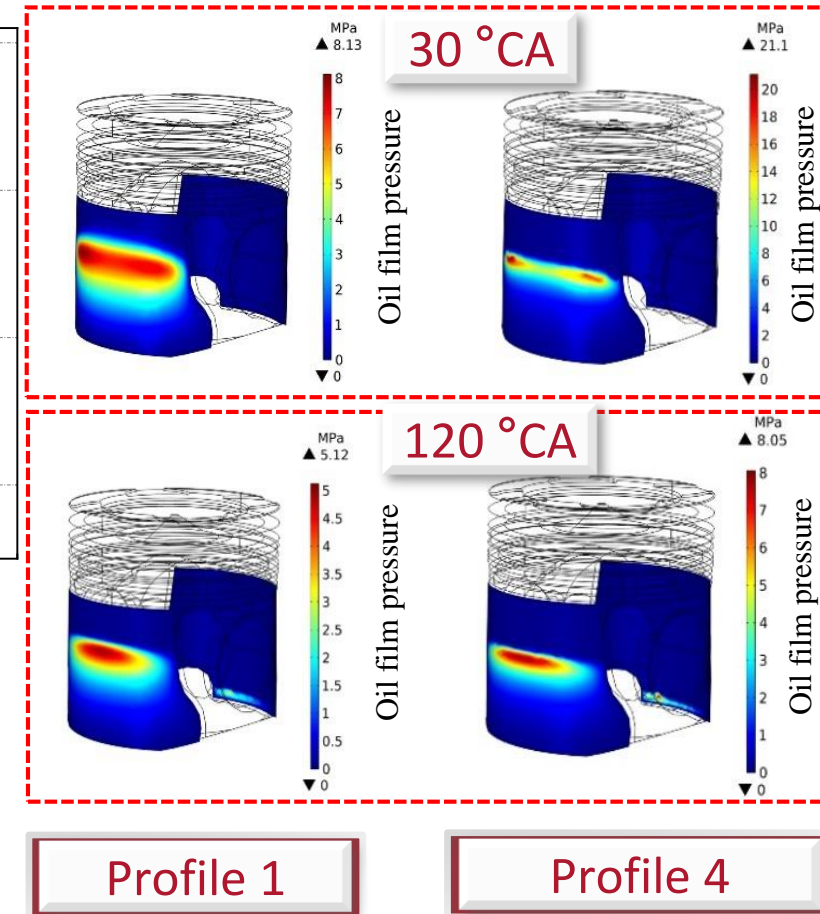
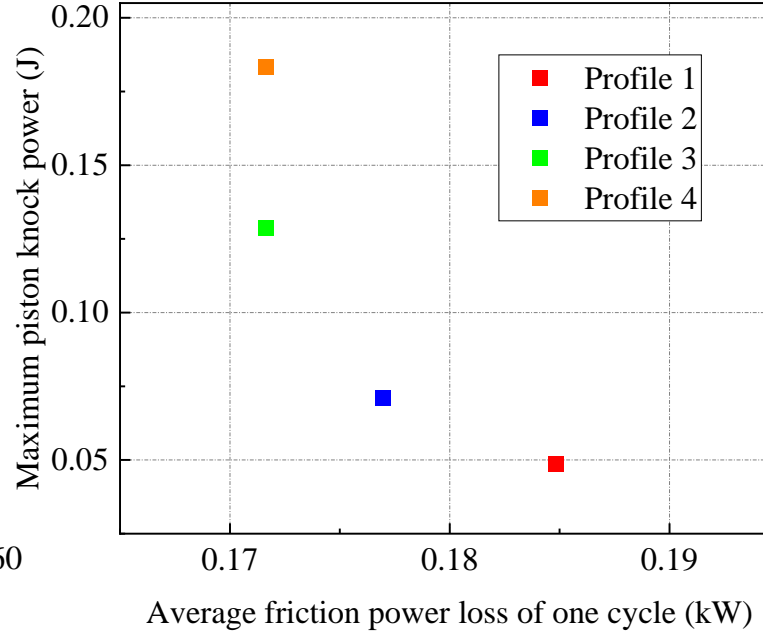
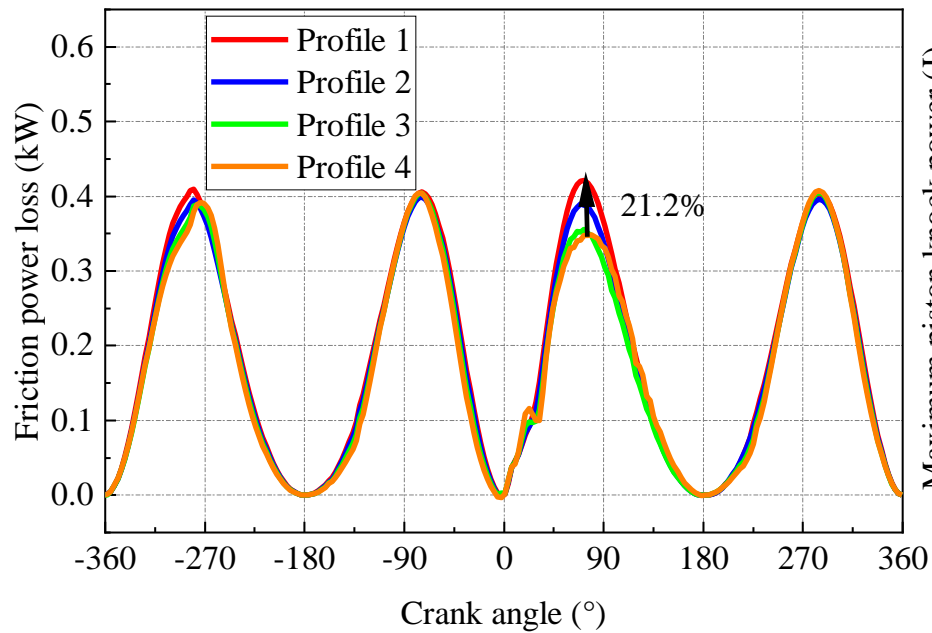
- During a cycle, the upper of piston skirt is in contact with the liner more frequently.
- Therefore, when reduce the radius of the upper skirt, the **secondary motion is more intense.**





Results & analysis --- Piston/Liner pairs

Influences of radial reductions on the upper skirt



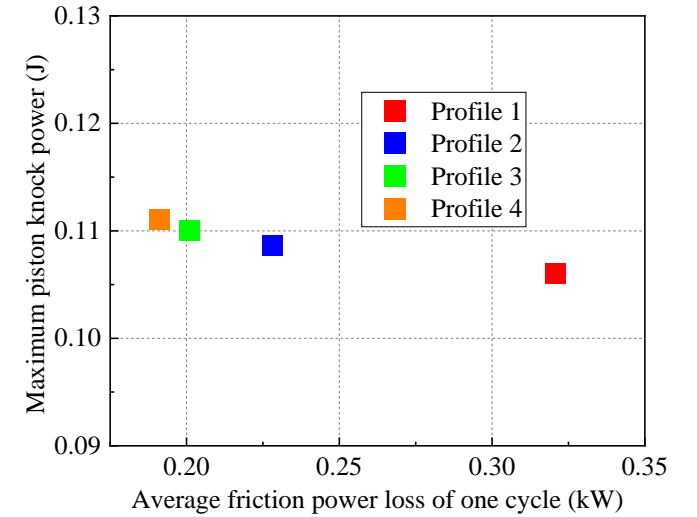
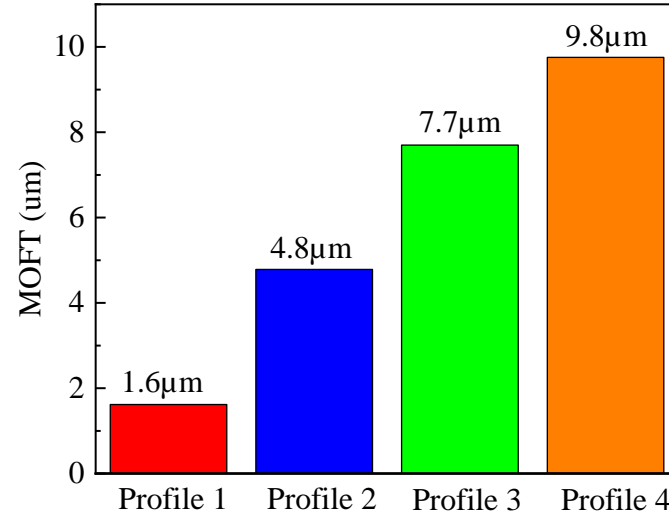
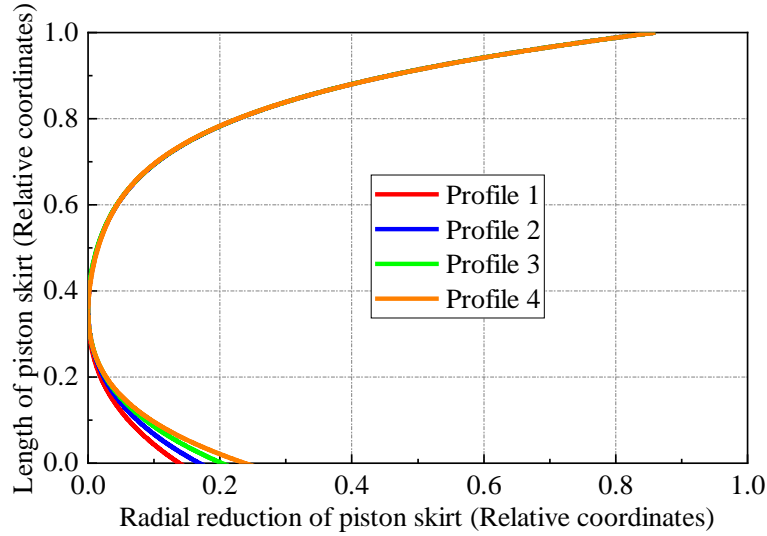
Reduce the radius of the upper skirt

- MOFT decreases and friction power loss decreases because of the smaller lubrication area.
- Piston knock power increases obviously.

Profile 1

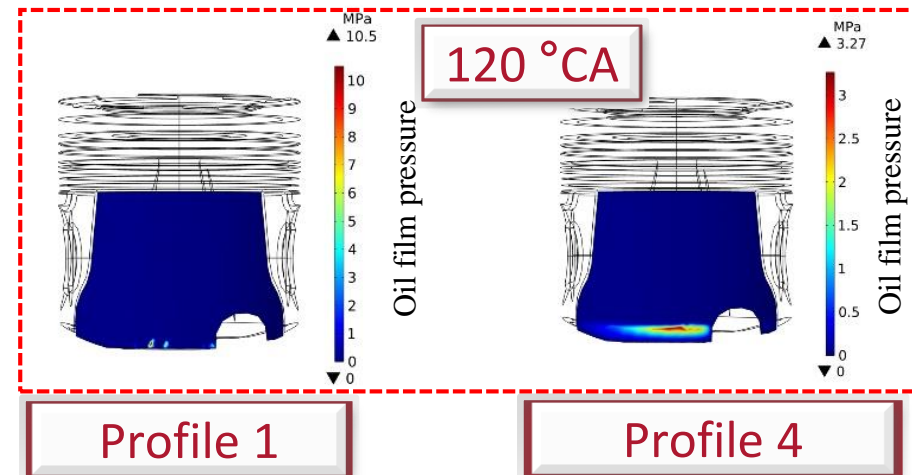
Profile 4

Influences of radial reductions on the lower skirt



Reduce the radius of the lower skirt

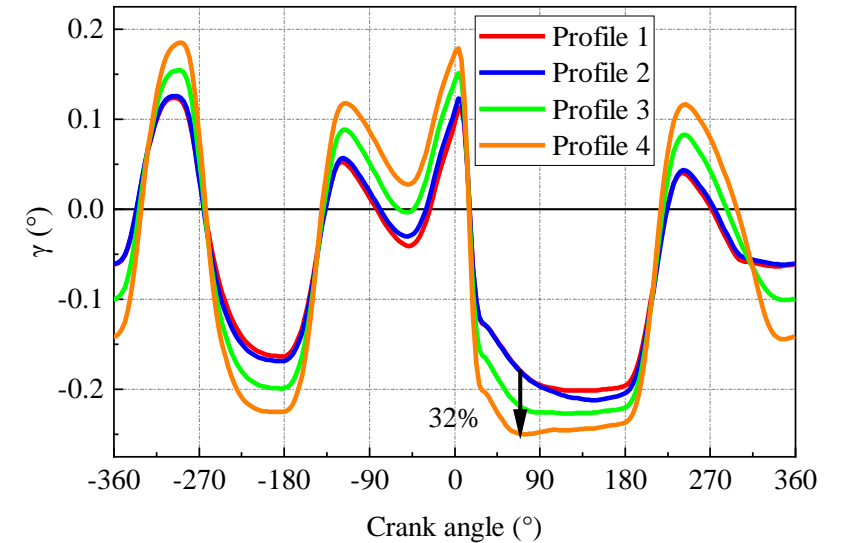
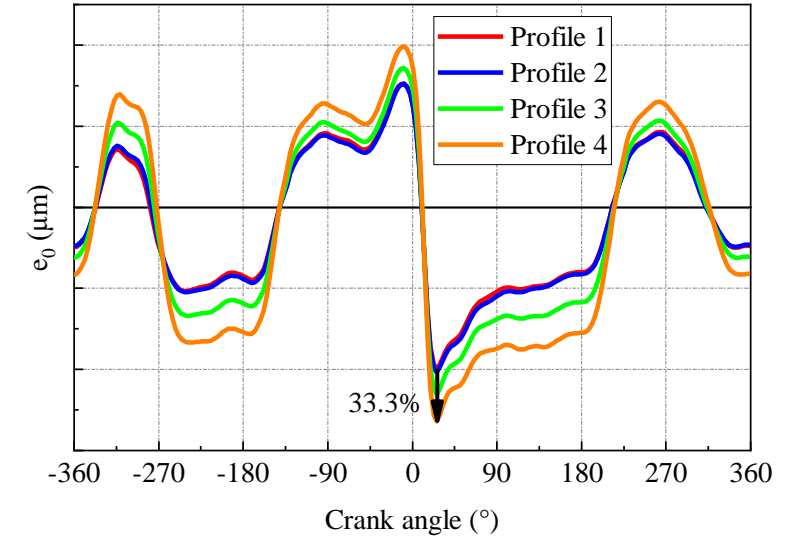
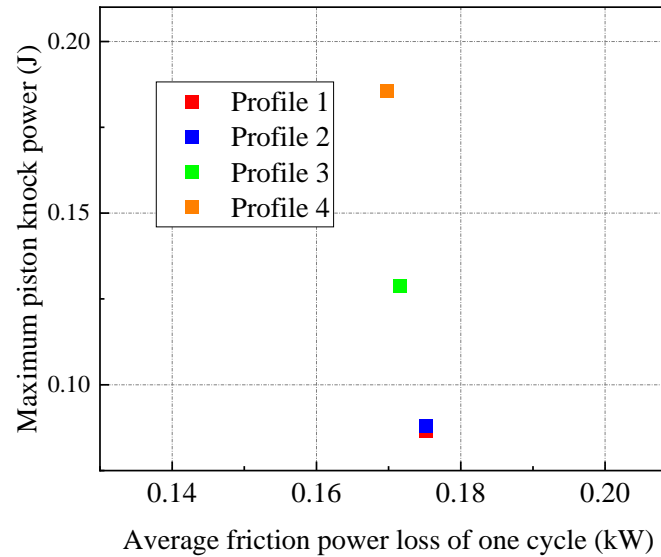
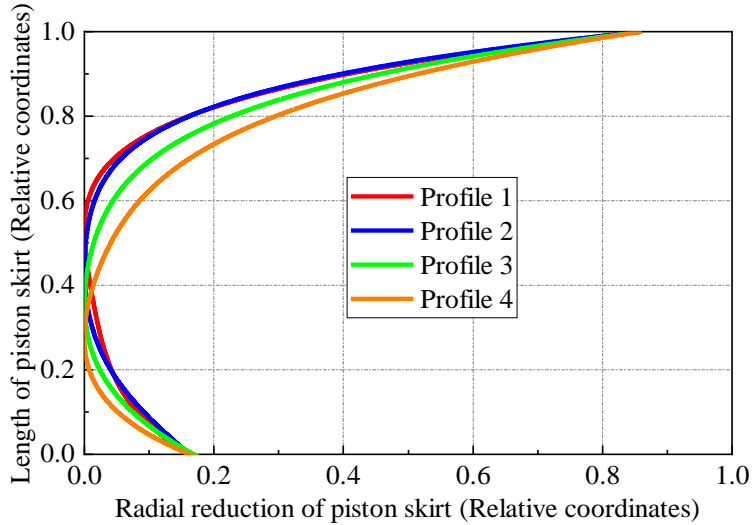
- Similar kinetic results
- MOFT increases and friction power loss decreases
- The knock power increases slightly





Results & analysis --- Piston/Liner pairs

Influences of bump position



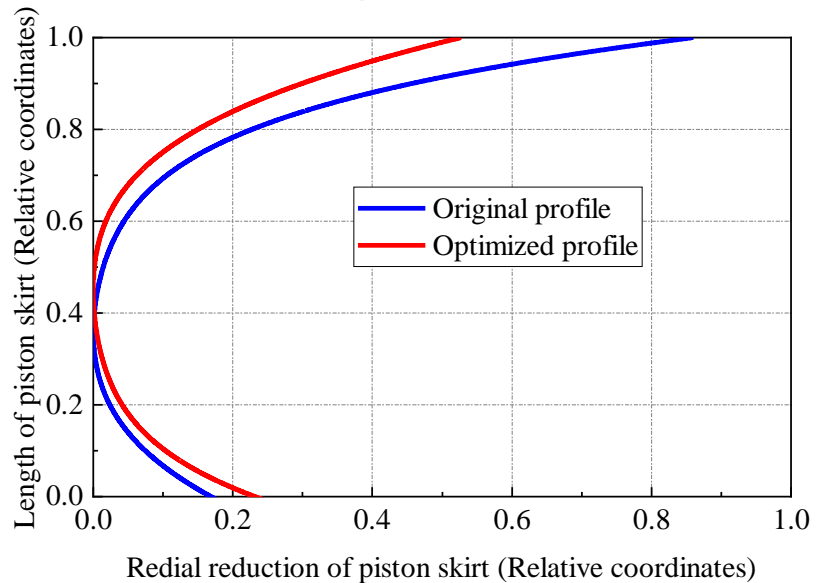
Move down the bump position

- Lubrication results are similar
- Piston knock power increases obviously
- Friction power reduced slightly



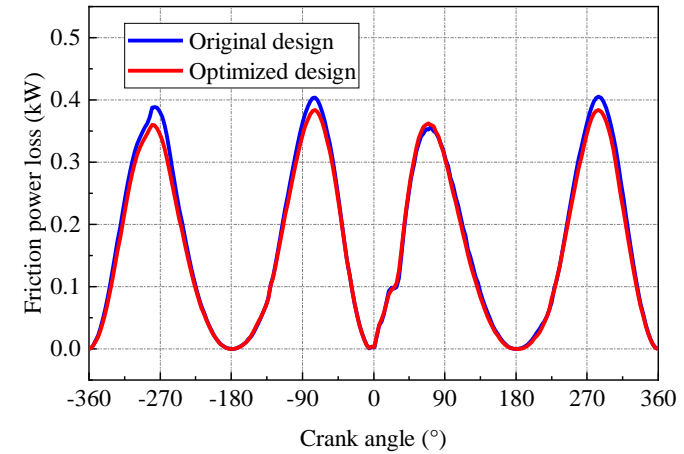
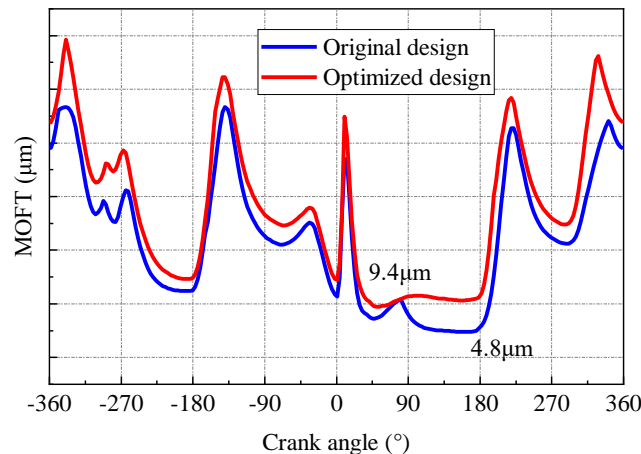
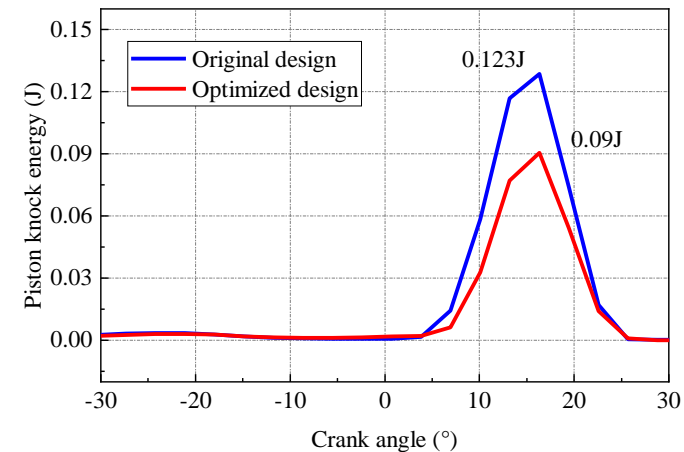
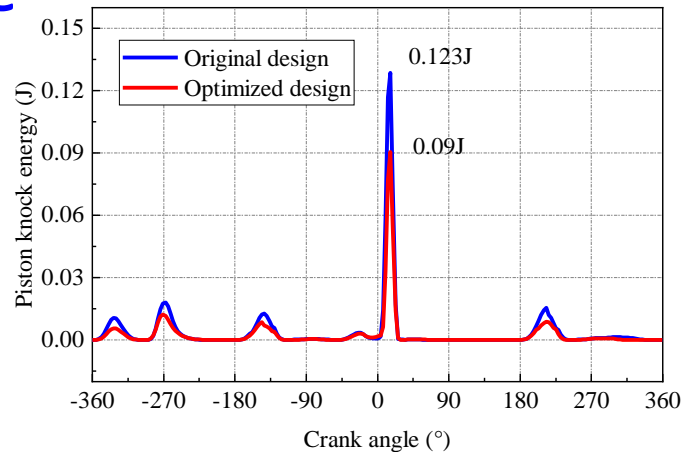
Results & analysis --- Piston/Liner pairs

Optimized design of piston skirt profile



Optimized design

- Piston's secondary motion has **weakened**, and piston knock energy **reduced by 27%**.
- MOFT **increases**, and average friction power loss of one cycle **reduced by 4.7%**.





PART 04

Conclusions





Conclusions

➤ *A new tribo-dynamic model*

A new tribo-dynamic model for the reciprocating friction pairs in engines is **proposed for the first time** by coupling the mixed lubrication model and the spatial rigid-flexible multibody system.

➤ *Effects of flexible bodies deformation*

More intense secondary motion, and **worse lubrication status for crosshead-guide pairs**, on the contrary, **better lubrication status for piston-liner pairs**.

➤ *Transmission characteristics of vibration signals*

Frame box vibration is mainly caused by the **slapping behavior of crosshead at TDC and the gas explosion pressure**. Vibration signal can be attenuated by oil film obviously, and by optimized contact profile of crosshead pad.

➤ *Influence of profile of piston*

Bump position mainly affects the knock power, the lower profile mainly affects the friction power, and the upper profile has a trade-off effects on the knock and friction power.



上海交通大學
SHANGHAI JIAO TONG UNIVERSITY

THANKS!